Progress In Electromagnetics Research B, Vol. 30, 117–133, 2011

EFFECTS OF GEOMETRY CONFIGURATIONS ON AMBIGUITY PROPERTIES FOR BISTATIC MIMO RADAR

H. W. Chen, X. Li, J. Yang, W. Zhou, and Z. W. Zhuang

Research Institute of Space Electronics Information Technology
Electronics Science and Engineering School
National University of Defense Technology
Changsha 410073, P. R. China

Abstract—Bistatic multiple-input multiple-output (MIMO) radar can improve the system performance for obtaining the waveform diversity and larger degrees of freedom (DoF), and effectively counteract the stealthy target for its transmit antennas and receive antennas separated placement. Similarly with the conventional bistatic radar, the geometry configurations of bistatic MIMO radar also play an important role in radar system's performance. Aimed at considering these effects of geometry configurations on the performance for bistatic MIMO radar, in this paper the extended ambiguity function is defined as the coherent cumulation of the matching output of all channels, where the information of the system geometry configuration is included in the received signal model. This new ambiguity function can be used to characterize the local and global resolution properties of the whole radar systems instead of only considering transmitted waveforms in Woodward's. In addition, some examples with the varying system configurations or target parameters are given to illustrate their effects, where the spatial stepped-frequency signal set (a quasi-orthogonal waveform set) is used. The simulation results demonstrate that the more approaching monostatic MIMO radar case, the better ambiguity properties of time-delay and Doppler for bistatic MIMO radar.

1. INTRODUCTION

Multiple-input multiple-output (MIMO) radar has gotten considerable attention in a novel class of radar system, where the term MIMO

Received 28 March 2011, Accepted 4 May 2011, Scheduled 8 May 2011
Corresponding author: Hao Wen Chen (chenhw@nudt.edu.cn).

refers to the use of multiple-transmit as well as multiple-receive antennas [1–19]. MIMO radar can transmit, via its antennas, multiple probing signals that may be correlated or uncorrelated with each other. There are two basic regimes of architecture considered in the current literature [6]. One is called statistical MIMO radar with widely separated antennas, which captures the spatial diversity of the target's radar cross section (RCS) [2, 3]. This spatial diversity gain can improve the target detection and estimation of variations parameters. The other is called coherent MIMO radar with colocated antennas, which can obtain the waveform diversity and larger degrees of freedom (DoF) to improve the target parameters estimation, parameter identifiability and much flexibility for transmit beampattern design [1, 4]. Furthermore, based on whether the transmit antennas and the receive antennas are separated or not, the coherent MIMO radar can be distributed into two classes. One is the bistatic MIMO radar [16]; the other is the monostatic MIMO radar [1]. The former is commonly with the quite different transmit antennas' locations from the receive antennas'. And all the transmit antennas and the receive antennas are colocated, respectively. Thus, the directions of the target to the transmit antennas and the receive antennas are almost the same in the far-field scenario, respectively. While monostatic MIMO radar is with all transmit and receive antennas colocated, then the directions of the target to all the antennas are almost the same in the far-field scenario. In our paper, we mainly consider the bistatic MIMO radar configuration. First, for this general antenna configuration, both the coherent processing gain and the spatial diversity gain can be achieved simultaneously. Second, we can consider monostatic MIMO radar as a special case of bistatic MIMO radar. At last, we want to show the performance of bistatic MIMO radar attended by many researchers [16, 20–23].

It is well-known that the classical ambiguity function was introduced by Woodward and is used to characterize the local and global resolution properties of time-delay and Doppler for narrowband waveforms [24]. Other authors have extended Woodward's ideas to larger classes of waveforms and whole radar systems [25, 26]. Normally, the classical ambiguity function couldn't illustrate the resolution properties of bistatic radar system appropriately for the effects of varying configuration. Then Tsao et al. proposed a new framework for ambiguity function for a bistatic radar configuration and showed the effects of geometry configurations on the performance of parameter estimation [27]. Recently, Antonio et al. [28] extended the radar ambiguity function to the MIMO radar case. It turns out that the radar waveforms affect not only the range and Doppler resolution but

also the angular resolution. They defined the MIMO radar ambiguity function as the expected value of the data loglikelihood function for the received data, which is viewed as a function of the whole radar system, geometry, waveforms, and target characteristic. In [29], some mathematical properties of the MIMO radar ambiguity function defined as in [28] are derived. And using these properties, a new algorithm for designing the orthogonal frequency-hopping waveforms is proposed. Here we mainly focus on the effects of geometry configurations of bistatic triangle [30] on the ambiguity properties of bistatic MIMO radar. And we define the bistatic MIMO radar ambiguity as the coherent cumulation of the matching output of all channels enlighten by [27]. So the geometry information is considered in this definition. It should be recognized that we are not defining a notion of ambiguity function that is vastly different from those of other authors. From statistical viewpoint, our definition is the somewhat similar to the one in [28]. Since it deems that the true target appears at the point with maximum probability in [28] while at the point with maximum coherent cumulation energy of the matching output in our definition, and both consider the ambiguity function from the received signals, which are different from the conventional ambiguity function from Woodward. A major difference between our definition and Antonio's [28] is that ours does not depend on the prior statistical information of the received signals.

This paper is arranged as follows. In Section 2, we give some preliminary elements. First, we review the geometry of bistatic MIMO radar from conventional bistatic radar, using two-dimensional (2-D) North-referenced coordinate system. Second, we derive the relationship between bistatic geometry with range and range rate, respectively, for a slowly fluctuating point target [27]. Third, we show the signal model for each channel. An ambiguity function for bistatic MIMO radar is given in Section 3, which includes the geometry information of system. In Section 4, the design of a quasi-orthogonal waveform set, i.e., spatial stepped-frequency signal set, is shown first. Then using this designed waveform set, it is shown that the effects of geometry configurations play an important role in the systems' ambiguity properties from the simulation results. A summary including conclusions is presented in Section 5.

2. PRELIMINARIES

2.1. Review Geometry of Bistatic MIMO Radar

In this subsection, we review the North-referenced coordinate system used in [30] to represent bistatic MIMO radar geometries.

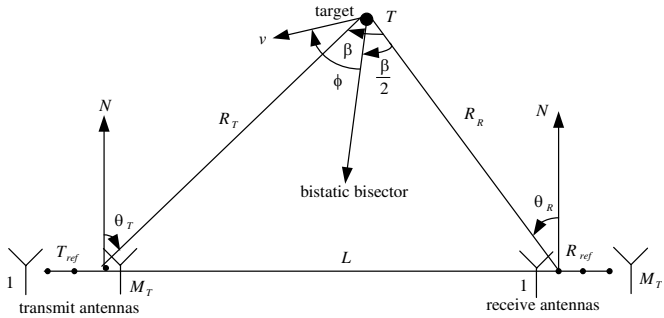

Figure 1. Bistatic MIMO radar geometry.

The North-referenced coordinate system is a 2-D coordinate system confined to the bistatic plane formed by the target T, and the reference transmit antenna T_{ref} and the reference receive antennas R_{ref}. Fig. 1 shows the coordinate system and its parameters. Connecting the reference transmit and receive antennas is the baseline whose length is L. When $L = 0$, bistatic MIMO radar reduce to the monostatic MIMO radar case. For the bistatic configuration, we can assume all the look angels for all transmitters to target are the same, called θ_T, and θ_R for all receivers. They are measured positive clockwise from the north of the coordinate system, and are restricted to the interval $[-\pi/2, 3\pi/2]$. The bistatic angle β is the angel at the apex of the bistatic triangle, and $\beta = \theta_T - \theta_R$. β is in the interval $[0, \pi]$ when the target is to the north of the baseline and is negative and in the interval $[-\pi, 0]$ when the target is to the south of the baseline. The line bisects the bistatic angel is called the bistatic bisector. R_T and R_R are the distances from the reference transmit antennas to target and from the reference receive antennas to target, respectively, their sum being the total range sum, i.e., $R = R_T + R_R$. We know the bistatic radar geometry can be completely specified in terms of any three of six parameters, R_T, R_R, θ_T, θ_R, L and R. Assume that R_R, θ_R and L are known, i.e., the receiver-centered operating region. This assumption is used in remainder work, and a similar procedure can be used to determine the bistatic geometry for other three parameters known, such as the transmitter-centered operating region (R_T, θ_T and L are known). The law of cosines applied to the bistatic triangle gives

$$R_T = \sqrt{R_R^2 + L^2 + 2R_R L \sin\theta_R} \tag{1}$$

Substituting (1) into $R = R_T + R_R$ and simplifying, we have

$$R = R_R + \sqrt{R_R^2 + L^2 + 2R_R L \sin\theta_R} \tag{2}$$

The law of cosines can also be written as

$$R_R^2 = R_T^2 + L^2 - 2R_T L \sin\theta_T \tag{3}$$

Using (1) to solve for θ_T, we have

$$\theta_T = \begin{cases} \sin^{-1}\frac{R_R\sin\theta_R + L}{\sqrt{R_R^2+L^2+2R_R L\sin\theta_R}}, & -\frac{\pi}{2} \le \theta_T < \frac{\pi}{2} \\ \pi - \sin^{-1}\frac{R_R\sin\theta_R + L}{\sqrt{R_R^2+L^2+2R_R L\sin\theta_R}}, & \frac{\pi}{2} \le \theta_T < \frac{3\pi}{2} \end{cases} \tag{4}$$

where $-\frac{\pi}{2} \le \sin^{-1}(\cdot) \le \frac{\pi}{2}$. Thus (1), (2) and (4) provide the remaining parameters of the bistatic geometry. In the next subsection, we will show the relationship of range and range rate with the geometry parameters.

2.2. Effects of Bistatic Geometry on Range and Range Rate

Assume that a slowly fluctuating point target with the velocity v. And the angle between the target velocity v and the bistatic bisector is ϕ, in Fig. 1, as measured in a positive clockwise direction from the bisector.

First, we consider the relationship between range and the known parameters of biastic geometry, i.e., R_R, θ_R and L. From (2), the total transmission time delay from the reference transmit antenna to the reference receive antenna as a function of R_R and θ_R is given by

$$\tau\left(R_R, \theta_R, L\right) = \frac{R_R + \sqrt{R_R^2 + L^2 + 2R_R L\sin\theta_R}}{c} \tag{5}$$

where c is the wave propagation speed. Clearly, (5) reduces to the monostatic case when $L = 0$.

Next, we consider the relationship between range rate and the known parameters. And for simplicity, we assume that the transmit and receive antennas are all stationary and the target is located north of the baseline; by symmetry, similar conclusion can be drawn for the case of the south of the baseline. Consider the first-order time-derivative of the total range. From Fig. 1 it is clear that

$$\frac{d}{dt}R_T = v\cos\left(\phi - \beta/2\right) \tag{6}$$

$$\frac{d}{dt}R_R = v\cos\left(\phi + \beta/2\right) \tag{7}$$

where $\frac{d}{dt}R_T$ is the projection of the target velocity vector onto the transmitter-to-target light of sight (LOS) [30], and similarly, $\frac{d}{dt}R_R$ is the projection of the target velocity vector onto the receiver-to-target LOS. Then we have

$$\frac{d}{dt}R = \frac{d}{dt}R_T + \frac{d}{dt}R_R = 2v\cos\phi\cos(\beta/2) \tag{8}$$

From the factor $\cos(\beta/2)$ we can see that the resulting range rate is smaller in the bistatic radar than in the monostatic case, when $\beta = 0$, (8) reduces to the monostatic case.

The dependence of $\cos(\beta/2)$ on the known parameters is shown in the following. From trigonometry

$$\cos(\beta/2) = \sqrt{\frac{1+\cos\beta}{2}} \tag{9}$$

And from the law of cosines,

$$\cos\beta = \frac{R_T^2 + R_R^2 - L^2}{2R_T R_R} \tag{10}$$

Using (1) to express R_T in (9), (10) becomes

$$\cos(\beta/2) = \sqrt{\frac{1}{2} + \frac{R_R + L\sin\theta_R}{2\sqrt{R_R^2 + L^2 + 2R_R L\sin\theta_R}}} \tag{11}$$

Then the Doppler shift for a given target velocity component along the bisector becomes

$$\omega_D(R_R, v, \theta_R, L) = 2\frac{\omega_c}{c} v\cos\phi \sqrt{\frac{1}{2} + \frac{R_R + L\sin\theta_R}{2\sqrt{R_R^2 + L^2 + 2R_R L\sin\theta_R}}} \tag{12}$$

where ω_c is the carrier frequency. It is clearly that (12) reduces to the monostatic case when $L = 0$.

2.3. Receive Antennas Output of Slowly Fluctuating Point Target

Consider a bistatic MIMO radar system with M_t transmit and M_r receive antennas. For simplicity, we assume that the transmit and receive antennas are located along the baseline. Furthermore, assume the distance between each transmit antenna with the reference transmit antenna is dt_k, $k = 1, \ldots, M_t$, similarly, the distance between each receive antenna with the reference receive antenna is dr_l, $l = 1, \ldots, M_r$. Assume that the transmitted signal of the kth transmitting antenna is given by $x_k(t) = \sqrt{\frac{P}{M_t}} s_k(t) = \sqrt{\frac{P}{M_t}} b_k(t)\exp(j\omega_c t)$, $k = 1, \ldots, M_t$, where $\int_{\mathrm{T_e}} |s_k(t)|^2 = 1$, P is the total transmitting energy, $b_k(t)$ is the complex envelop, and T_e is the waveforms' duration. Normalization by M_t makes the total energy independent of the number of transmitters. Disregarding the propagation loss, the

waveform transmitted by the kth antenna and received by the lth receive antenna can be written as

$$r_{kl}(t) \cong \sqrt{\frac{P}{M_t}}\zeta b_k(t-\tau_{kl}) \cdot \exp(j(\omega_c - \omega_{kl})t) \tag{13}$$

where ζ is the unknown complex target reflectivity, which is proportional to the RCS of the target. Using (5), τ_{kl} can be written as

$$\tau_{kl} = \tau(R_R, \theta_R, L) + \tau_k + \tau_l \tag{14}$$

where $\tau_k = \frac{dt_k \cos\theta_T}{c}$ and $\tau_l = \frac{dr_l \cos\theta_R}{c}$, and τ_{kl} and ω_{kl} are the total transmission time delay and Doppler shift for the kth transmit antenna-target-lth receive antenna channel, respectively. $\frac{dt_k \cos\theta_T}{c}$ is the difference of time delay from the kth transmit antenna to target with the one from the reference transmit antenna to target, $\frac{dr_l \cos\theta_R}{c}$ is defined in the similar way.

We assume that the transmitted waveforms are narrowband so that the complex envelop of the waveforms are insensitive to the motion of the target. And for the bistatic MIMO radar configuration, the time delay in the envelop for all channels can be approximate to the time delay of the reference transmit antenna-target-reference receive antenna channel, i.e., $\tau_{kl} \approx \tau(R_R, \theta_R, L)$; the Doppler shift for all channels can be the same as the Doppler shift of the reference transmit antenna-target-reference receive antenna channel, i.e., $\omega_{kl} \approx \omega_D(R_R, v, \theta_R, L)$. Then (13) can be rewritten as

$$\begin{aligned} r_{kl}(t) \;=\; & \sqrt{\frac{P}{M_t}}\zeta b_k(t-\tau(R_R,\theta_R,L)) \\ & \cdot \exp(j(\omega_c - \omega_D(R_R, v, \theta_R, L))\; t) \end{aligned} \tag{15}$$

From above equation, we can see that the received signal depend on the geometry configuration of radar system heavily. For conventional bistatic radar, its configuration employs only a single transmit antenna and a single receive antenna. Then the waveform received by the receive antenna can be written as

$$r(t) = \sqrt{P}\zeta b(t-\tau(R_R,\theta_R,L)) \cdot \exp(j(\omega_c - \omega_D(R_R, v, \theta_R, L))t) \tag{16}$$

3. AMBIGUITY FUNCTION FOR BISTATIC MIMO RADAR

The conventional ambiguity function just determine limitations on radar resolution in range and range rate only considering the transmitting waveform [24]. For bistatic MIMO radar, the geometry configuration of the triangle constituted by the transmit antennas,

target and receive antennas is a very important factor for system ambiguity performance. Then ambiguity function including the geometry information can illustrate the more actual performance of bistatic MIMO radar system. The authors in [27] gave the ambiguity function for conventional bistatic radar expressed as

$$\begin{aligned}&\mathrm{A}\left(R_{R_H}, R_{R_a}, v_H, v_a \middle| \theta_R, L\right)\\&\propto \left| \int_{-\infty}^{\infty} b\left(t-\tau_a\left(R_{R_a}, \theta_R, L\right)\right) b^*\left(t-\tau_H\left(R_{R_H}, \theta_R, L\right)\right)\right.\\&\left.\cdot \exp\left(-j\left(\omega_{D_a}\left(R_{R_a}, v_a, \theta_R, L\right) \ -\omega_{D_H}\left(R_{R_H}, v_H, \theta_R, L\right)\right) t\right) dt \right|^2 \quad (17)\end{aligned}$$

where the subscripts a and H are used to denoted the actual and hypothesized value of the parameters associated with the target, respectively, and $\{\cdot\}^*$ denotes the complex conjugate operator. For notational brevity, we omit the argument R_{R_H} or R_{R_a}, v_H or v_a, θ_R and L of τ_a, τ_H, ω_{D_a} and ω_{D_H} in remainder paper. This ambiguity function is the result of matching the received signal corresponding to the actual total delay and Doppler. Similarly, we can define the ambiguity function for bistatic MIMO radar as the coherent cumulation of the matching output of all channels, i.e.,

$$\begin{aligned}&\mathrm{A}_{\mathrm{MIMO}}\left(R_{R_H}, R_{R_a}, v_H, v_a \middle| \theta_R, L\right)\\&= \left| \sum_{i=1}^{M_r} \sum_{k=1}^{M_t} \int_{-\infty}^{\infty} r_{kl}\left(t\right)\big|_{\left(R_{R_a}, v_a, \theta_R, L\right)} \ r_{kl}^*\left(t\right)\big|_{\left(R_{R_H}, v_H, \theta_R, L\right)} dt \right|^2\\&\propto \left| \sum_{i=1}^{M_r} \sum_{k=1}^{M_t} \int_{-\infty}^{\infty} b_k\left(t-\tau_a\right) b_k^*\left(t-\tau_H\right) \exp\left[j\left(\omega_{D_H}-\omega_{D_a}\right) t\right] dt \right|^2 \quad (18)\end{aligned}$$

where τ and ω functions include the geometry information, see (5) and (12), respectively. Intuitively speaking, our ambiguity function definition deems that the true target appears at the point with maximum coherent cumulation energy of the matching output. The difference between in (17) and (18) is mainly from the waveform diversity with bistatic MIMO radar.

4. NUMERICAL EXAMPLES

4.1. Orthogonal Waveform Models

In this subsection, the spatial stepped-frequency signal set is designed, which satisfies the "quasi-orthogonal" condition. The kth transmit

antenna emits the waveform in the form

$$x_k(t) = \sqrt{\frac{P}{M_t T_e}} rect(t) \exp\left(j2\pi\left(f_c + c_k \Delta f\right) t\right), \quad k = 1, \ldots, M_t \quad (19)$$

where

$$rect(t) = \begin{cases} 1, & 0 \le t \le T_e \\ 0, & \text{otherwise} \end{cases}$$

and f_c is the base frequency, $c_k \Delta f$ is the increase value of carrier frequency for the kth signal. With loss generality, we assume that $c_k = k - 1$ holds in the remainder paper (see Fig. 2). Denoting t_k as the propagation time from the kth transmit antenna to the target and then arrive at the receive antennas. In the far-field scene, the correlation function of the kth and lth transmitting signals can be expressed as (without loss generality, assuming $t_k \ge t_l$)

$$\begin{aligned} r_{k,l}(t) &= \int_{-\infty}^{\infty} x_k(t - t_k) x_l^*(t - t_l) dt \\ &= \int_{t_k}^{T_e + t_r} \frac{P}{M_t T_e} \left(\exp j2\pi \left[f_c\left(t_l - t_k\right)\right.\right. \\ &\quad \left.\left. + \Delta f\left(l t_l - k t_k\right) + \Delta f\left(l - k\right)\right] t\right) dt \\ &\approx \frac{P}{M_t T_e} \exp\left(j2\pi\left[f_c\left(t_l - t_k\right) + \Delta f\left(l t_l - k t_k\right)\right]\right) \\ &\quad \cdot \int_0^{T_e} \exp\left(j2\pi \Delta f\left(l - k\right) t\right) dt \qquad (20) \\ &= \frac{P}{M_t} \exp\left(j2\pi\left[f_c\left(t_l - t_k\right) + \Delta f\left(l t_l - k t_k\right)\right]\right) \\ &\quad \cdot \frac{\sin \pi \Delta f\left(l - k\right) T_e}{\pi \Delta f\left(l - k\right) T_e} \qquad (21) \end{aligned}$$

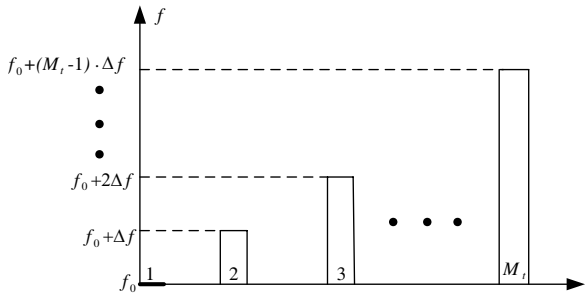

Figure 2. Spatial stepped-frequency signal set for MIMO radar.

It is worth to note that we have a approximate consideration in (20): $t_k \leq t \leq T_e + t_l \xrightarrow{app} 0 \leq t \leq T_e$ for $T_e \gg t_k, t_l$, where $A \xrightarrow{app} B$ denotes that A is approximate of B. To guarantee the orthogonality of the kth and lth transmitting signals, we have $r_{k,l}(t) = 0$, $\forall k, l = 1, \ldots, M_t$, and $k \neq l$. Then we can get the following results

$$\Delta f\,(l-k)\,T_e \in Z, \quad \forall k, \quad l = 1, \ldots, M_t, \quad \text{and} \quad k \neq l \tag{22}$$

4.2. Examples Illustration

In the following examples, we focus on the effects on the ambiguity function by the system geometry. R_R and v as the independent arguments of ambiguity function are given for a variety of bistatic

Table 1. Specification of a variety of bistatic configurations and target parameters.

Case index	θ_R (degree)	L (km)	R_{R_a} (km)	v_a (m/sec)
case 1	90	2000	1300	200
case 2	45	2000	1300	200
case 3	0	2000	1300	200
case 4	−45	2000	1300	200
case 5	−90	2000	1300	200
case 6	−45	2000	1300	100
case 7	−45	2000	3300	200
case 8	−45	500	1300	200
case 9	−45	0	1300	200

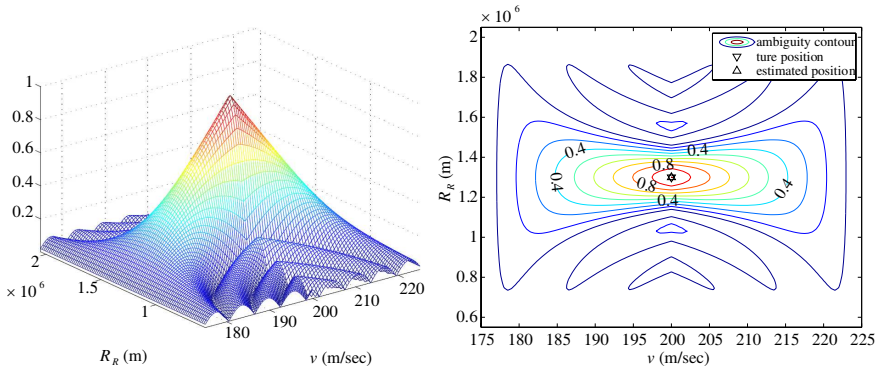

Figure 3. Bistatic MIMO radar ambiguity function plots for case 1.

configurations. The receiver-centered operating region is adopted in the geometry considered [30], shown in Table 1. In the similar manner, geometry effects can be examined for transmitter-centered operating regions. Especially, in case 6, bistatic MIMO radar reduces to monostatic MIMO radar case for $L = 0$.

Assume a bistatic MIMO radar with 4 transmit antennas and 4 receive antennas, the inter-elements paces of transmit antennas and receive antennas are both half of wavelength, respectively. Here we use the signals designed in Section 4.2. Here we give a set of orthogonal signals for MIMO radar with 4 transmit and 4 receive antennas: $P = 1$, $T_e = 1\,\text{ms}$, $f_c = 1\,\text{GHz}$ and $\Delta f = 10\,\text{kHz}$ in (19).

In Figs. 3–11 (all the leftward sub figures are the ambiguity surface in terms of total delay and Doppler, and the rightward sub figures are the corresponding equal-height plots, respectively), we

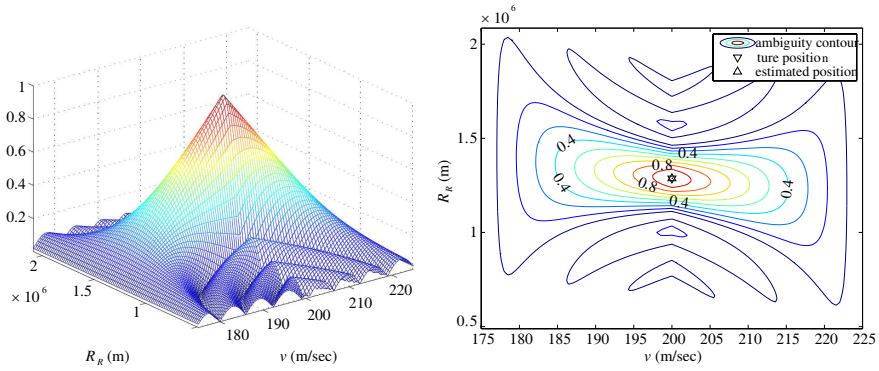

Figure 4. Bistatic MIMO radar ambiguity function plots for case 2.

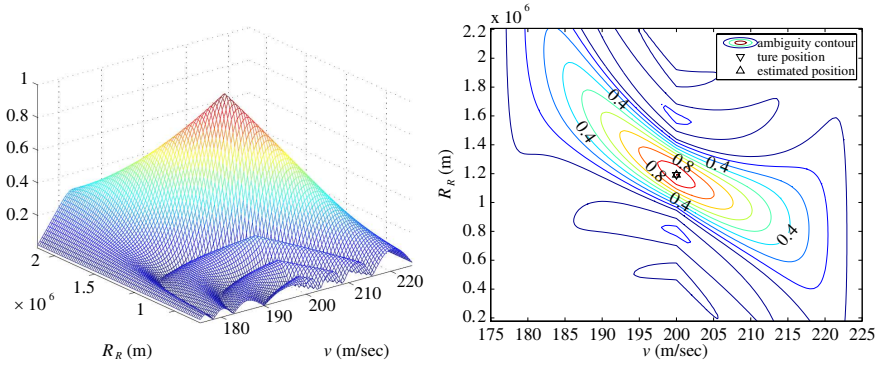

Figure 5. Bistatic MIMO radar ambiguity function plots for case 3.

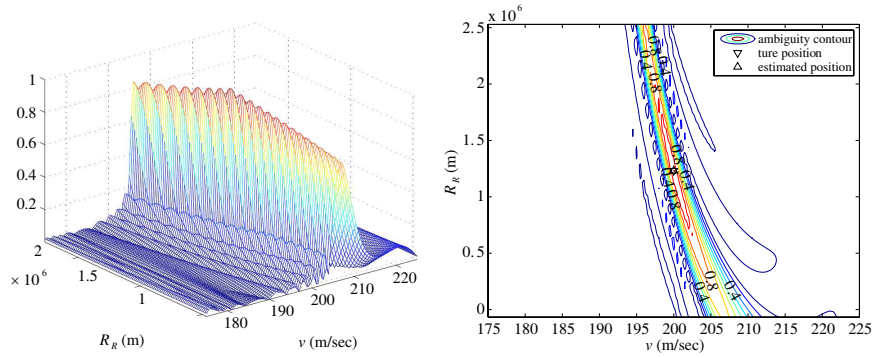

Figure 6. Bistatic MIMO radar ambiguity function plots for case 4.

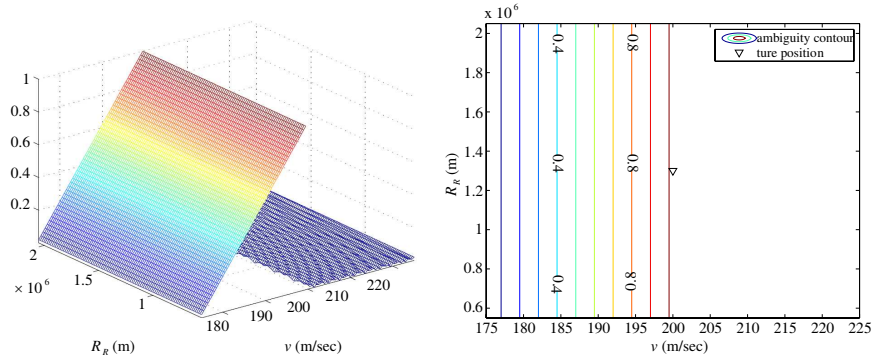

Figure 7. Bistatic MIMO radar ambiguity function plots for case 5.

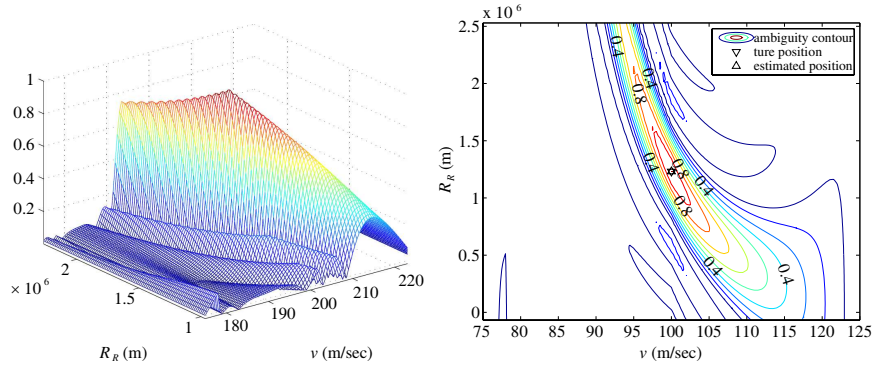

Figure 8. Bistatic MIMO radar ambiguity function plots for case 6.

give the plots of $\mathrm{A}_{\mathrm{MIMO}}\left(R_{R_H}, R_{R_a}, v_H, v_a|\theta_R, L\right)$ corresponding to the geometry configuration or different target parameters cases in Table 1, respectively. In other words, Figs. 3–10 are the ambiguity

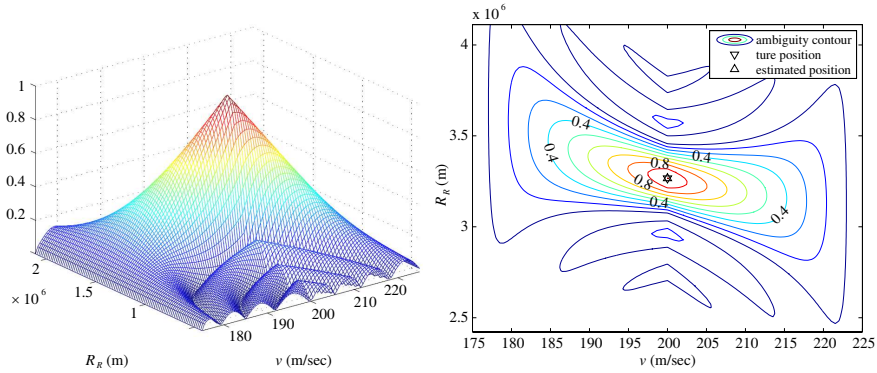

Figure 9. Bistatic MIMO radar ambiguity function plots for case 7.

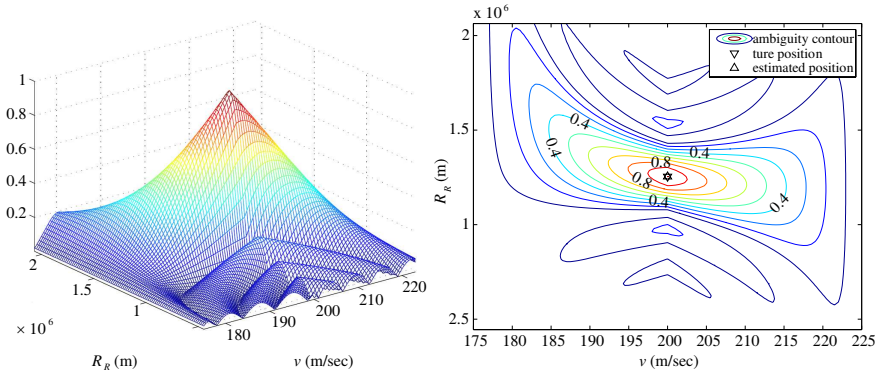

Figure 10. Bistatic MIMO radar ambiguity function plots for case 8.

function plots corresponding to the bistatic MIMO radar with different configurations or different target parameters and Fig. 11 is the ambiguity function plots corresponding to the monostatic MIMO radar. We can see that the geometry configurations play an important role in the systems' ambiguity properties. For case 1, the system configuration is somewhat similar to the monostatic MIMO radar in case 9 (since in case 1 the transmit antennas, the receive antennas and the target are collinear and the target is located at the same side of all the antennas, this is somewhat similar with the monostatic MIMO radar case), then they have the similar ambiguity function plots between Fig. 3 and Fig. 11. In Figs. 4–6 and 8–10, we find that the true target parameters can be estimated with the worse performance than monostatic MIMO case in Fig. 10. However, Fig. 7, corresponding to case 5 in Table 1, shows that the resolution is totally lost when the target is on the baseline. From Figs. 6, 9, 10 and 11,

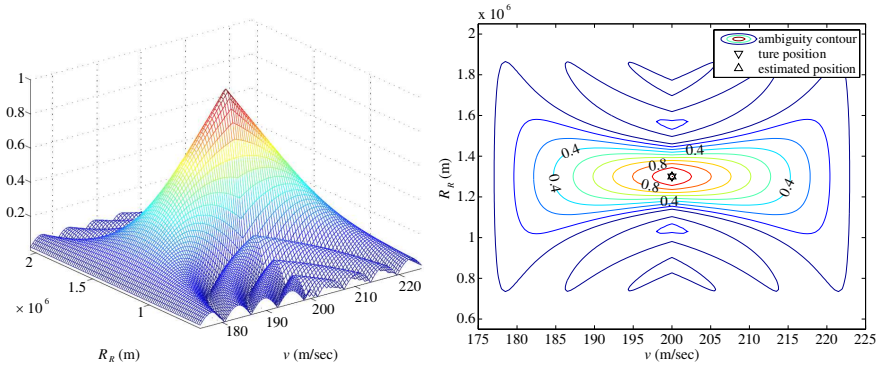

Figure 11. Monostatic MIMO radar ambiguity function plots for case 9.

corresponding to cases 4, 7, 8 and 9 in Table 1, respectively, we find that the better ambiguity performance can be gotten by approaching monostatic MIMO radar configuration (it is worth noting that the geometry configuration with the longer target range in case 7 or the shorter baseline length in case 8 is more approaching the monostatic MIMO radar case (case 9) than one in case 4).

In conclusion, the bistatic MIMO radar configuration is more approaching the monostatic MIMO radar case, the better ambiguity performance will be gotten.

5. CONCLUSION AND DISCUSSION

This paper presented a new framework of the ambiguity function for a bistatic MIMO radar. The effects of geometry configurations of bistatic triangle on ambiguity properties were emphasized. We defined the ambiguity function for a bistatic MIMO radar as the coherent cumulation of the matching output of all channels, where the information of the system geometry configuration is included in the received signal model. It was also worth to note that the bistatic MIMO radar ambiguity function needs to be considered with respect to an appropriate reference point. Here we considered the receiver-centered operating region. The examples, using the spatial stepped-frequency signal set, demonstrated the fact that the bistatic geometry plays an important role in the shape of ambiguity function. Furthermore, the resolution was totally lost when the target is on the baseline. In a word, the better ambiguity performance of bistatic MIMO radar can be obtained from a more approaching monostatic MIMO configuration.

It is worth noting that bistatic MIMO configuration is needed in some practical applications for obtaining its spatial diversity gain, such

as the case of effectively detecting a stealthy target. Furthermore, it is worth noting that effects of geometry configurations cannot be given when using the conventional ambiguity function disregarding the geometry information. The methodology presented here can be used to evaluate the capability of transmitted waveform set and the system performance for bistatic MIMO radar.

As in array signal processing [31, 32], the antennas placement strategy for MIMO radar (a multiple antennas frame), which we did not consider here, also plays an important role in the performance of systems. Honestly speaking, we mainly focused on the effects of the geometry configuration of bistatic triangle on the ambiguity properties for bistatic MIMO radar in this paper. And the optimal antennas placement strategy will be further studied in near future.

ACKNOWLEDGMENT

The authors wish to thank the anonymous reviewers for their efforts in providing comments that have helped to significantly enhance the quality of this paper. The work of X. Li was supported in part by a grant from National Science Fund for Distinguished Young Scholars under No. 61025006.

REFERENCES

1. Li, J. and P. Stoica, "MIMO radar with colocated antennas: Review of some recent work," *IEEE Signal Process. Mag.*, Vol. 24, No. 5, 106–114, 2007.
2. Haimovich, A. M., R. S. Blum, and L. Cimini, "MIMO radar with widely separated antennas," *IEEE Signal Process. Mag.*, Vol. 25, No. 1, 116–129, 2008.
3. Krairiksh, M., P. Keowsawat, C. Phongcharoenpanich, and S. Kosulvit, "Two-probe excited circular ring antenna for MIMO application," *Progress In Electromagnetics Research*, Vol. 97, 417–431, 2009.
4. Qu, Y., G. S. Liao, S. Q. Zhu, X. Y. Liu, and H. Jiang, "Performance analysis of beamforming for MIMO radar," *Progress In Electromagnetics Research*, Vol. 84, 123–134, 2008.
5. Mallahzadeh, A. R., S. Es'haghi, and A. Alipour, "Design of an E-shaped MIMO antenna using IWO algorithm for wireless application at 5.8 GHz," *Progress In Electromagnetics Research*, Vol. 90, 187–203, 2009.
6. Li, J. and P. Stoica, Eds., *MIMO Radar Signal Processing*, Wiley-Interscience, New York, 2008.

7. Fishler, E., A. Haimovich, R. Blum, D. Chizhik, L. Cimini, and R. Valenzuela, "MIMO radar: An idea whose time has come," *Proc. IEEE Radar Conf.*, 71–78, 2004.
8. Abouda, A. A. and S. G. Haggman, "Effect of mutual coupling on capacity of MIMO wireless channels in high snr scenario," *Progress In Electromagnetics Research*, Vol. 65, 27–40, 2006.
9. Fishler, E., A. Haimovich, R. Blum, D. Chizhik, L. Cimini, and R. Valenzuela, "Performance of MIMO radar systems: Advantages of angular diversity," *Proc. 38th Asilomar Conf. Signals, Syst. Comput.*, Vol. 1, 305–309, Pacific Grove, CA, 2004.
10. Huang, Y., P. V. Brennan, D. Patrick, I. Weller, P. Roberts, and K. Hughes, " FMCW based MIMO imaging radar for maritime navigation," *Progress In Electromagnetics Research*, Vol. 115, 327–342, 2011.
11. Fishler, E., A. Haimovich, R. Blum, D. Chizhik, L. Cimini, and R. Valenzuela, "Spatial diversity in radarsmodels and detection performance," *IEEE Trans. Signal Processing*, Vol. 54, 823–838, 2006.
12. Bliss, D. W. and K. W. Forsythe, "Multiple-input multiple-output (MIMO) radar and imaging: Degrees of freedom and resolution," *Proc. 37th Asilomar Conf. Signals, Syst. Comput.*, Vol. 1, 54–59, Pacific Grove, CA, 2003.
13. Chou, H.-T., H.-C. Cheng, H.-T. Hsu, and L.-R. Kuo, "Investigations of isolation improvement techniques for multiple input multiple output (MIMO) WLAN portable terminal applications," *Progress In Electromagnetics Research*, Vol. 85, 349–366, 2008.
14. Forsythe, K., D. Bliss, and G. Fawcett, "Multiple-input multiple-output (MIMO) radar: Performance issues," *Proc. 38th Asilomar Conf. Signals, Syst. Comput.*, Vol. 1, 310–315, Pacific Grove, CA, 2004.
15. Fuhrmann, D. R. and G. S. Antonio, "Transmit beamforming for MIMO radar systems using partial signal correlation," *Proc. 38th Asilomar Conf. Signals, Syst. Comput.*, 295–299, 2004.
16. Bencheikh, M. L. and Y. Wang, "Combined ESPRIT-Rootmusic for DOA-DOD estimation in polarimetric bistatic MIMO radar," *Progress In Electromagnetics Research Letters*, Vol. 22, 109–117, 2011.
17. Bekkerman, I. and J. Tabrikian, "Target detection and localization using MIMO radars and sonars," *IEEE Trans. Signal Processing*, Vol. 54, 3873–3883, 2006.

18. Robey, F. C., S. Coutts, D. Weikle, J. C. McHarg, and K. Cuomo, "MIMO radar theory and exprimental results," *Proc. 38th Asilomar Conf. Signals, Syst. Comput.*, Vol. 1, 300–304, Pacific Grove, CA, 2004.
19. Abouda, A. A., H. M. El-Sallabi, and S. G. Haggman, "Effct of antenna array geometry and ULA azimuthal orientation on MIMO Channel properties in urban city street grid," *Progress In Electromagnetics Research*, Vol. 64, 257–278, 2006.
20. Jin, M., G. Liao, and J. Li, "Joint DOD and DOA estimation for bistatic MIMO radar," *Signal Processing*, Vol. 89, 244–251, 2009.
21. Yan, H., J. Li, and G. Liao, "Multi-target identification and localization using bistatic MIMO radar systems," *EURASIP J. Adv. Signal Processing*, 2008.
22. Bencheikh, M. L., Y. D. Wang, and H. Y. He, "Polynomial root finding technique for joint DOA DOD estimationin bistatic MIMO radar," *Signal Processing*, Vol. 90, 2723–2730, 2010.
23. Chen, J. L., H. Gu, and W. M. Su, "A new method for joint DOD and DOA estimation in bistatic MIMO radar," *Signal Processing*, Vol. 90, 714–718, 2010.
24. Woodward, P., *Probability and Information Theory, with Applications to Radar*, Pergamon, New York, 1957.
25. Rendas, M. J. D. and J. M. F. Moura, "Ambiguity in radar and sonar," *IEEE Trans. Signal Processing*, Vol. 46, No. 2, 294–305, 1998.
26. Urkowitz, H., C. Hauer, and J. Koval, "Generalized resolution in radar systems," *Proc. IRE*, Vol. 50, 2093–2105, Oct. 1962.
27. Tsao, T., M. Slamani, P. Varahney, D. Weiner, H. Schwarzlander, and S. Borer, "Ambiguity function for a bistatic radar," *IEEE Trans. Aerospace Electron. Syst.*, Vol. 33, No. 3, 1041–1051, 1997.
28. Antonio, G. S., D. R. Fuhrmann, and F. C. Robey, "MIMO radar ambiguity functions," *IEEE J. Sel. Topics Signal Processing*, Vol. 1, No. 1, 167–177, 2007.
29. Yang, C. C. and P. P. Vaidyanathan, "MIMO radar ambiguity properties and optimization using frequency-hopping waveforms," *IEEE Trans. Signal Processing*, Vol. 56, No. 12, 5926–5936, 2008.
30. Willis, N. J., *Bistatic Radar*, SciTech Publishing Inc., 2005.
31. Hawkes, M. and A. Nehorai, "Effects of sensor placement on acoustic vector-sensor array performance," *IEEE J. Oceanic Eng.*, Vol. 24, 33–40, 1999.
32. Baysal, U. and L. Moses, "On the geometry of isotropic arrays," *IEEE Trans. Signal Processing*, Vol. 51, 1469–1478, 2003.